School of Chemistry

Thermionic Emission from Sc-O-terminated Diamond

Poppy Pearce

This thesis is submitted in partial fulfilment of the requirements for the Honours Degree of BSc at the University of Bristol.

Supervisor: Professor Paul May
Second Assessor: Professor Neil Fox
Third Assessor: Professor Neil Allan

Abstract

Thermionic emission has the potential to be applied in thermionic energy converters (TECs) to convert heat directly to electricity. This technology could then be implemented in solar energy devices in order to produce renewable energy. Diamond has been considered a promising material for emitters in this field due to its overall robustness and conductivity properties. This project explored Sc-O as a new surface termination and its ability to enhance the thermionic emission properties of diamond.

A 10x10 mm sample was produced as the emitter which consisted of nitrogen doped nanocrystalline diamond grown onto a Mo substrate. The same sample was then terminated firstly with hydrogen and its thermionic capability was tested with bespoke testing equipment. The same sample was then freshly terminated with Sc-O and was tested again for comparison.

The H-terminated sample lacked temperature stability and achieved a highest emission value during its first profile of 0.586 mA, after which emission decreased in subsequent profiles due to the desorption of the hydrogen at temperatures exceeding 600 °C and the sample not being freshly terminated between profiles. In comparison the Sc-O-termination showed greater stability and reached its maximum emission output in the final testing of 2.569 mA, showing emission does not decrease in successive profiles.

From the initial investigation of Sc-O as a suitable surface termination it would appear it has desirable characteristics, however further testing needs to be carried out, potentially at even higher temperatures.

Acknowledgements

Firstly, thanks go to Paul May for the proposal of the project and his input into my work throughout the year. I am also grateful to Neil Fox for additional advice and ideas, enhancing my understanding of the topics that I have explored.

I also owe a huge thank you to Ramiz Zulkharnay for his ongoing supervision, guidance and patience throughout the project. Without him I would not have completed this project with such a good understanding of how to perform all the laboratory techniques and understanding of the theory behind them.

A final thanks goes to the University of Bristol Diamond lab, which was a welcoming work environment with all individuals both interested and assisting in each other's research.

Table of Contents

Table of Figures

Glossary of terms

Acronym	Meaning
TEC	Thermionic energy converter
NEA	Negative electron affinity
PEA	Positive electron affinity
CBM	Conduction band minimum
PETE	Photon enhanced thermionic emission
HPHT	High pressure high temperature
CVD	Chemical vapour deposition
TMO	Transition metal oxide
NDD	Nitrogen doped diamond
MWCVD	Microwave chemical vapour deposition
SEM	Scanning electron microscopy

1. Introduction

This report explores thermionic emission using diamond as an emitter. Thermionic emission devices are used in many modern applications; they provide a means to convert heat directly into electricity. They are appealing devices due to their size, scalability, and ability to utilise solar radiation allowing them to potentially become a renewable energy source[1].

Diamond shows promise as a thermionic emitter due to many of its properties, for example, correct doping allows the material to become conducting, its surface can possess a negative electron affinity, and many other properties which make diamond ideal for the cathode material.

1.1 Thermionic Emission

1.1.1 The History of Thermionic Emission

The discovery of thermionic emission, the process by which electrons are liberated from a surface when provided with sufficient thermal energy, can be, in part accredited to the observations of Edison and his work on carbon filament incandescent lamps. Edison observed a blackening of the glass walls inside the lamp, which suggested carbon was being transferred there from the filament. Upon further investigation it was then suggested that the carbon atoms which were 'carried' were negatively charged and only those arising from the negative end of the filament could reach the glass. Edison's work did not explain this science, but it prompted the works of other scientists and led to a better understanding of thermionic emission[2]. The first thermionic diode reported was in Flemings 1890 paper; combinations of these works led to the first application of thermionic emission as a detector of radio signals[3].

Unfortunately, during the work developing thermionic emission, experimental conditions were not perfect, and this led to conflicting ideas and the disregarding of several works. During the early 20th century there were two theories competing to provide an explanation for the emission of electrons. The first supported that it was an underlying feature of the cathode material and increasing the thermal energy naturally resulted in increased kinetic energy, the other theory explained that the electrons were emitted due to a chemical reaction between the cathode material and residual gases. In the first case lower pressure is favoured for better emission, in the latter higher pressure is desirable. In order to resolve this debate, there needed to be experiments performed and repeated under better vacuum conditions. It was not until 1913 that the first and now accepted theory was good and viable under better vacuum conditions. A notable discovery that came during this time is from the work of Wehnelt, who showed any material can emit electrons if heated to a sufficient temperature without breaking down[4]. Further work was done after this time which allowed an accurate equation to be established to describe the phenomenon.

1.1.2 Theory of Thermionic Emission

The equation for emission took its final form in 1923 after Dushman's adaptations to the equation first produced by Richardson several years earlier. This equation is known by multiple names, but in this paper shall be referred to as the Richardson-Dushman equation.

$$J = A_R T^2 e^{\left(-\frac{\varphi}{kT}\right)} \quad (1)$$

In the equation, J denotes emission current, A_R is the Richardson constant which will be further discussed, T is the absolute temperature of the emitting material, φ is the work function and k is the Boltzmann constant[5]. By analysing the format of this equation, particularly the exponential component, it is evident that emission will increase with a temperature increase, until kT exceeds the work function. Another consequence of this is that slight changes in the work function will significantly affect emission. Ideal conditions for maximum current would be high temperature and

low work function, although the temperature will be limited by the melting point of the material. The Richardson constant, A_R, causes much confusion and disagreement amongst scientists. A value of 120 A cm^{-2} K^{-2} is widely accepted using equation (2).

$$A_0 = \frac{4\pi mqk^2}{h^3} \tag{2}$$

Here, *m* and *q* represent the mass and charge of the electron, respectively, and *h* is Planck's constant[6]. Experimental data show the value of A_R is often very different to the ideal value of A_0 and can, in fact, vary from 0.35 to 160 A $cm^{-2}K^{-2}$. This is important, as it means A_R can vary over several orders of magnitude. Potential causes of this are impurities absorbed onto the surface, the surface not being uniform and surface films[7].

In order to provide more accurate experimental data, a correction can be applied to determine A_R from A_0, using a correction factor λ_R which is material specific and has been determined for several materials.

$$A_R = A_0\lambda_R \tag{3}$$

Confusion arises here as it is not always stated what form of the Richardson constant is being used as the subscripts 0 and R are often interchanged.

1.2 Thermionic Energy Convertors

1.2.1 Overview of Thermionic Energy Converters

An important application of thermionic emission is in thermionic energy converters (TECs). Here, electricity is produced by the conversion of heat energy. The electrons released from a heated cathode travel across an interelectrode gap where they are collected by a cooler anode. Having a connection between the two electrodes allows current to flow from the anode back to cathode[8].

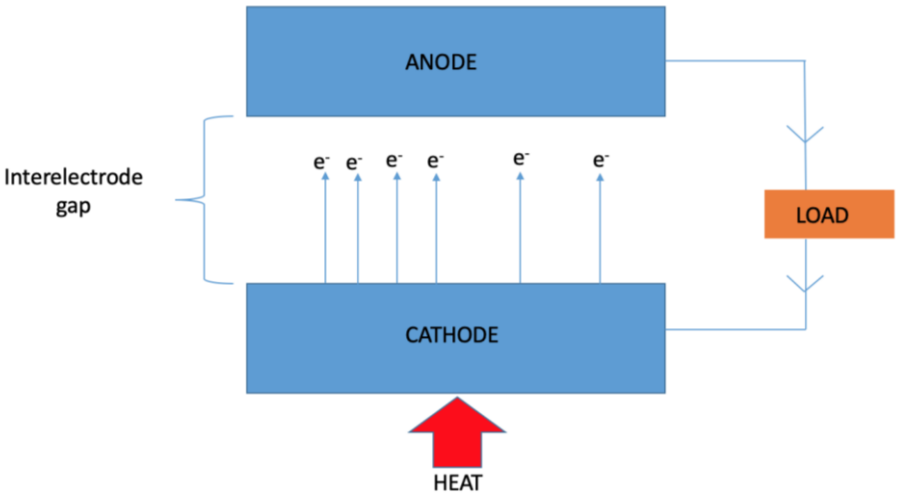

Figure 1 - A schematic diagram of thermionic energy conversion.

The interelectrode gap may be either a vacuum or vapour gap. A vacuum gap consists of a highly evacuated space. This type of TEC suffers from the problem of the space-charge effect. If the gap is instead filled with gas the space-charge effect is lessened by the presence of positive ions, which means the vapour TEC can have better efficiency[9]. In both cases, while the system is in operation, a negative charge will build up on the anode from the collection of electrons, inducing a potential

difference between the two electrodes. By connecting the electrodes, this voltage can drive a current through a load; the cycle is continuous as the electrons return to the cathode where they can be reemitted. Thus, the TEC acts as a heat engine, continuously converting heat energy into electricity.

1.2.2 Electron Emission

Electron extraction from metals has long been studied in order to find the most efficient technique. Methods include thermionic emission, which is the focus of this report; this involves ejection of electrons from the surface via high temperatures; photoemission, which uses photons to liberate electrons from the surface; and field emission, which uses electric fields to lower the energy barrier for electron emission[10].

1.2.3 Practical limitations of TECs

Work on TECs began properly in the mid-1900s. Their science continues to be of interest as the goal is to make them as efficient as possible using the best materials available.

1.2.3.1 Work Function

The work function of a material is the minimum energy required for electrons to be liberated from the surface[11]. In an ideal TEC, the work function of both the cathode and anode would be as low as possible whilst maintaining at least a 1 eV difference between the two. This has proven to be a problem in developing thermionic energy converters as there is a lack of materials with both a low work function and high thermal stability[9]. Methods have been researched in order to create cathodes with lower work functions, in particular by coating the emitter with a low-work function layer. A low work function of 1.7 eV was achieved on a polycrystalline-silicon carbide substrate after having barium oxide deposited on a tungsten adhesion layer on the surface. This system was able to run at temperatures between 900-1400 K for several hours indicating stability[12]. This study demonstrated potential for more robust electrodes.

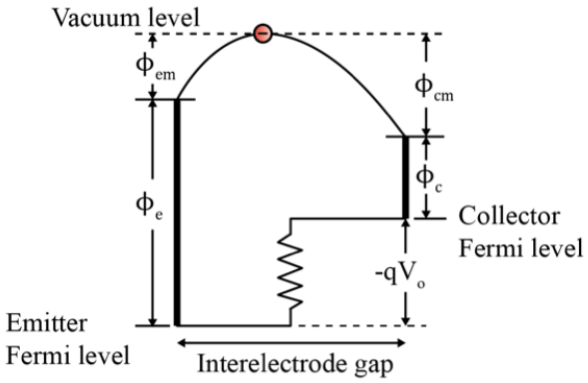

Figure 2 - An energy diagram of a TEC. Φ_e and Φ_c are the work function of emitter and collector respectively. Φ_{em} and Φ_{cm} are the additional barriers of the space charge effect of the emitter and collector, respectively. The voltage difference between the electrodes is denoted V_0. The electron charge is shown by $-q$[9].

1.2.3.2 Space-Charge

Another issue that has arisen during the development of TECs is known as the space-charge effect, a build-up of electrons in the interelectrode gap[13]. This effect drastically reduces the efficiency of the TEC. As electrons are emitted, some will not possess sufficient energy to travel to the anode. These electrons will be attracted back to the cathode, which is now slightly positive due to the loss of electrons. This causes an electron 'cloud' to form in the vacuum gap near the cathode, which inhibits

current flow[14]. This effect creates an additional energy barrier for emission. It was first recognised in the early 20th century, but solutions have come several years later as an interest in TECs grew[3].

The addition of positive ions, e.g. Cs^+, into the vacuum gap improves the efficiency[15]. Although their addition neutralises the negative charge, the ions also take away energy from the system during ionisation[16]. Reducing the gap between the electrodes reduces the effect of space-charge. However, this is not very useful as it makes it difficult to maintain the large temperature differences between the electrodes necessary for TEC operation. It does, however, remove the need for a plasma to be placed in the interelectrode gap[17]. When micron-scale (<10 μm) gaps are used, the TEC can become a lot more efficient. However, if the gap becomes too small, quantum tunnelling may occur[18].

1.2.3.3 Electron Affinity

Another possible modification is altering the surface of the emitter material. It has been demonstrated that materials which possess a negative electron affinity (NEA) can also improve the efficiency of emitters. Smith investigated hydrogen-terminated diamond as a possible material for this process. Due to the material possessing NEA, the surface vacuum level lies lower than the conduction band minimum (CBM) of the material. This material, and others of its kind, allow for only electrons with sufficient kinetic energy, and therefore the least affected by the space charge effect, to be emitted and reach the collector[13].

Figure 3 shows the key differences in positive electron affinity (PEA) and true NEA and where the vacuum band, denoted E_{vac} lies in the respective systems. This makes it clear why emission is greater when the NEA surface is present. True NEA, as exhibited in hydrogen-terminated diamond, is displayed when the vacuum level has a lower energy value than the CBM[19]. Effective NEA occurs when the vacuum level is below the CBM in the bulk of the material, but when electrons from this level arrive at the surface their energy is often lower than that necessary for emission[20].

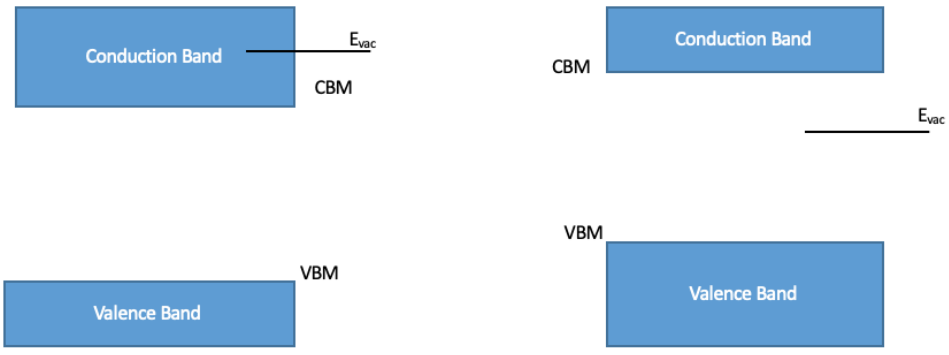

Figure 3 - Band diagrams for a PEA surface (left) and an NEA surface (right).

1.2.4 Theory Surrounding TECs

1.2.4.1 TEC Efficiency

Naturally, of key importance when developing TECs is achieving the most efficient model. It has already been seen that for optimum performance, materials with low work functions are favourable, whilst maintaining a difference of 1 eV between the cathode and anode. The material also needs to have good thermal stability. Research and solutions so far still have not achieved the efficiencies

which these systems have the ability to reach[21] due to many issues, including, but not limited to, the practical considerations mentioned above.

Efficiency is measured by the Carnot equation, which has a few differing forms. In its simplest it can be shown as the equation below[22].

$$\eta_{Carnot} = 1 - \frac{T_c}{T_h} \tag{4}$$

Here, the efficiency is dependent on the temperature of the anode, T_c and the temperature of the cathode, T_h only. It is evident that in order to increase the efficiency either the temperature of the anode needs to be decreased, but this is limited by cooling rates, or that of the cathode needs to be increased, but this is limited by the thermal stability of the material.

A more complex equation can be used which accounts better for the overall efficiency of the TEC, including more terms and considering more forms of energy-loss within the system. In equation (5) *Jc is* the emission current from the cathode, V_c is the potential of the cathode, V_a is the potential of the anode, V_w is the voltage loss that occurs due to connecting of electrodes to a load, *R* represents radiation from cathode to anode and *H* is heat conduction[23].

$$\eta_{Carnot} = \frac{J_c(V_c - V_a - V_w)}{R + H + J_c\,(V_c + 2kT)} \tag{5}$$

1.2.4.2 Increasing Efficiency

Many of the solutions to creating a more efficient TEC involve solving the issues associated with space-charge, however, some include modifications to the TEC to resolve other problems.

New techniques are constantly evolving as new discoveries are made. One proposed idea is changing the surface of one or both electrodes. Adding texture to the cathode surface can increase the surface area for emission. This is done by patterning the surface with micron-scale ridges and has been shown to be effective[24]. For the anode, reflection of electrons needs to be reduced or eliminated in order to improve collection and overall efficiency. The etching of pores and other irregular surface features designed to capture electrons proved to increase collection efficiency, as did reducing the work function of the electrode using a Cs-O coating on the surface[25]. These are promising for the development of better TECs.

Decreasing the work function will always be a key idea when trying to enhance the performance of TECs. Finding and synthesising materials with this property is at the forefront of research in this area. Diamond is a promising material for this reason, as it can be engineered to possess a surface dipole layer[21].

1.2.5 Photon Enhanced Thermionic Emission

Photon enhanced thermionic emission (PETE) explores a relatively new technique for the conversion of electrons to electricity. PETE involves utilising solar radiation in order to enhance the thermionic emission of electrons from a semiconducting cathode material.

First, the electrons are excited to the cathode conduction band by solar radiation. They then diffuse through the cathode to the surface, and any surface electrons with energies greater than that of the electron affinity can be emitted and subsequently collected[26].

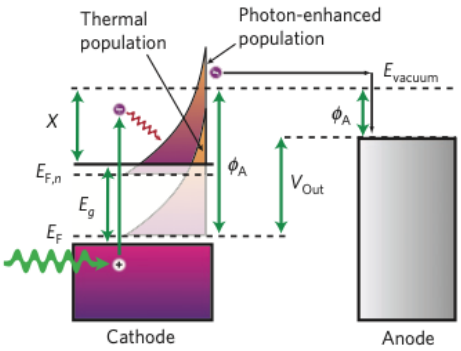

Figure 4 - Energy diagram of the PETE process. The conduction-band population is increased, and the device is able to harvest both photon and thermal energy[26].

Higher efficiency and output than conventional TEC devices can be achieved by this method. The energy barrier for emission is lowered and liberation of electrons can occur at lower temperatures than are usually required. Another benefit is the ability to have the anode at a higher temperature than in typical TECs allowing for better waste management, which can utilise the unused thermal energy in a secondary converter, without the creation of a reverse current[27].

1.2.6 Applications of Thermionic Energy Converters

A particular interest arose in using TECs in the 1960s as the race for space travel was on. Both the US and the then Soviet Union explored the use of TECs in their respective programmes. The Soviet Union continued this work and developed the Topaz-I and Topaz-II thermionic reactors. Currently there is more research occurring into its uses, and the US Navy is looking into the benefit of its use in submarines[28].

Interestingly thermionic energy conversion is being considered as a greener energy source. Scientists are trying to reinvent ideas around TECs as a viable energy source in developing countries that lack the necessary infrastructure for other power sources.

1.3 Diamond

1.3.1 Properties of Diamond

The physical properties of diamond are very interesting and have great potential for use in thermionic emission. Naturally occurring diamond is unfortunately not fit for use in this practice due to its expense, scarceness and variability between materials[29].

Diamond is the best material in many ways, it has the highest thermal conductivity at room temperature (2200 W m^{-1} K^{-1})[30], it is the hardest material known, it has excellent optical properties (has transmission of wavelengths from the ultraviolet to microwave region), it is also a wide-bandgap semiconductor (E_{gap} = 5.47 eV)[31].

Modifications to diamond can give additional qualities making it more suitable as an emission surface. When terminated with hydrogen a negative electron affinity surface is created. This induces a small surface dipole, attracting electrons to the surface where they will be more easily expelled[32]. Other surface terminations have been tested and can give a similar affect when the dipole created has the positive charge on the outermost layer.

1.3.2 Synthesis of Diamond

Diamond synthesis has been investigated for over 50 years. There have been obstacles in the synthesis due to the thermodynamic instability of diamond in comparison to other allotropes of carbon. Although the difference in the standard enthalpies of graphite and diamond only deviate by 2.9 kJ mol^{-1}, a huge activation barrier limits the two phases interconverting at room temperature[29]. This does, however, provide reason for why, once formed diamond will not spontaneously convert to graphite and is kinetically stable. Clearly, a synthesis method needs to be employed in which diamond is the thermodynamically stable allotrope.

From Figure 5 it is evident that the higher the temperature, the higher the corresponding pressure needs to be for diamond to be the most stable form. During the early research into diamond synthesis, a high-pressure, high-temperature (HPHT) technique was utilised for growth. This only produced small crystals which are used for mechanical applications like cutting and grinding[33].

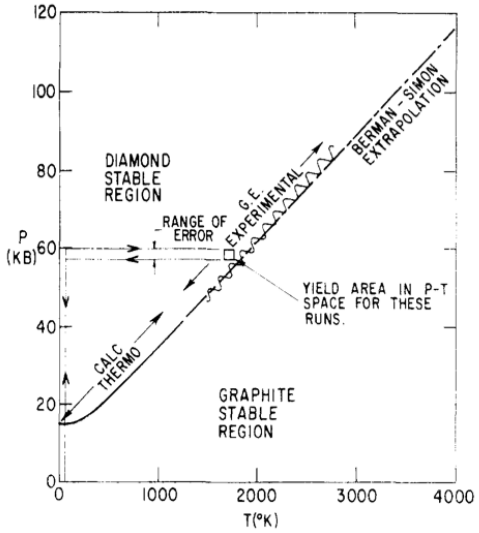

Figure 5 - Graphite-Diamond equilibrium curve[34].

More recently, chemical vapour deposition (CVD) techniques have been investigated and advanced. These show promise for the synthesis of diamond films which can be used in practical applications. CVD requires hydrogen gas and a carbon-containing gas, usually methane. These gases need to be activated to form their respective radicals, which is usually done in one of two ways. The first way is by using a very hot metal filament, with temperatures exceeding 2000˚C and the temperature of the substrate above 700˚C[35]. The other way is by using a microwave plasma, the plasma enables the formation of atomic hydrogen. Today, the microwave plasma is the more common practice as it uses lower pressure conditions making it cheaper and more accessible. These methods usually result in hydrogen-terminated diamond, creating the surface dipole. However, including other gases in the process can induce doping of the surface material[35].

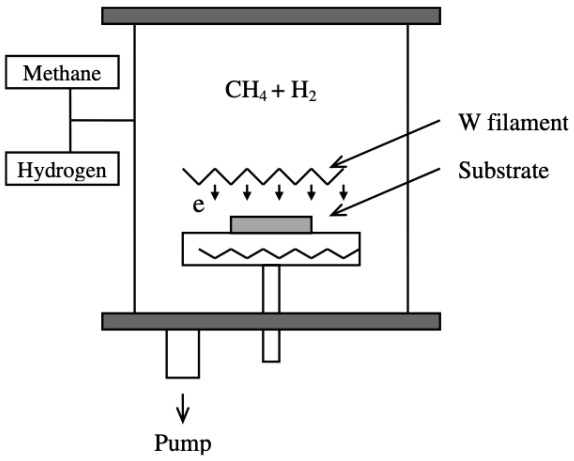

Figure 6 - Diagram of a hot filament reactor[36].

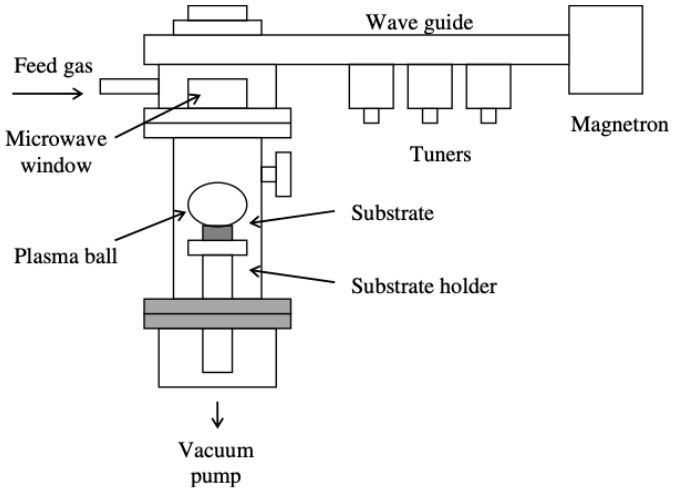

Figure 7 - Diagram of a microwave plasma reactor[34].

1.3.3 Doping of Diamond

During diamond growth, impurities can be added into the vacuum chamber or into the plasma. These additions are incorporated into the diamond lattice and create energy levels within the band gap, reducing its magnitude. As a result of the reduced band gap, less energy is required to promote electrons from the valence to conduction band, allowing the material to become a useful semiconductor. This process is known as doping, and there are two types, p-type and n-type[37].

1.3.3.1 p-type doping

To synthesis p-type diamond in the lab requires a boron containing molecule to be added into the gas mixture during either hot filament or plasma CVD[37]. Boron-doped diamond forms a band at ~0.37 eV above the valence band maximum; this is an acceptor level. At room temperature, electrons from the valence band can be easily promoted to this level, allowing the material to conduct[38].

1.3.3.2 n-type doping

For n-type doping, either nitrogen or phosphorus can be introduced. They provide donor bands at 1.7 eV[39] and 0.67 eV[40] below the CBM, respectively. Although this process is harder to achieve due to the rigid nature of the sp^3 hybridised diamond lattice and the larger size of most n-type dopants[39].

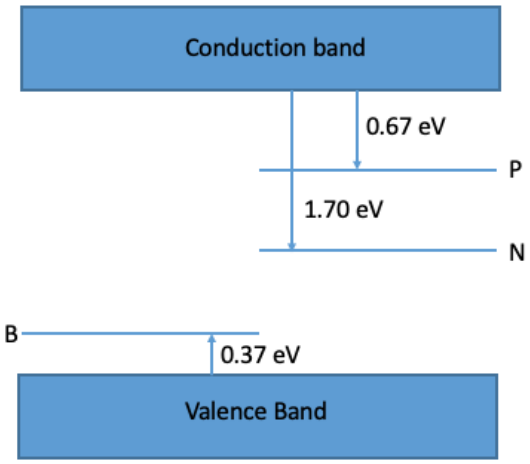

Figure 8 - Energy levels given by doping diamond.

1.3.4 Termination of Diamond

Termination of diamond is another way to enhance its electronic properties. As dopants struggle to diffuse into the bulk, these modifications to the surface may be the best way to increase the emission from diamond.

1.3.4.1 Hydrogen Termination

A hydrogen-terminated diamond surface is easily achieved by CVD due to the excess of hydrogen in the gas mixture. This surface is assumed to have a surface dipole due to the slight difference in electronegativities of the carbon and hydrogen. This surface possesses a negative electron affinity (NEA, see section 3.3.3 earlier)[41], of -1.30 eV[42], removing the energy barrier for emission for those electrons residing in the conduction band.

The main issue with hydrogen-terminated diamond is its thermal instability. Desorption of H from the surface occurs at relatively low temperatures (above 600˚C)[43]. The remaining surface now possesses a PEA which causes a significant reduction in emission. A more stable termination that provides both NEA and high-temperature stability is necessary for TEC applications.

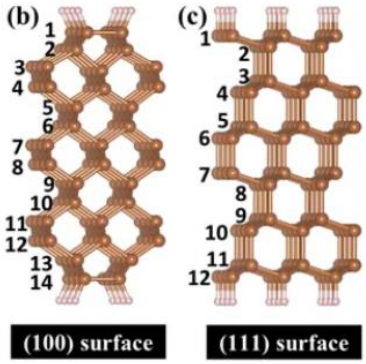

Figure 9 - Diamond surfaces. Hydrogen atoms are represented in white and carbon in brown[44]. Numbers showing increasing slab-layers from the surface.

1.3.4.2 Oxygen Termination

A solely oxygen-terminated diamond surface is not useful in the interests of emission. Oxygen is a more electronegative element than carbon and so the surface dipole is negative at the outermost layer, repelling surface electrons back into the bulk[45]. The oxygenated surface provides a PEA of 1.70 eV[42]. It is useful in order to create a metal oxide on the surface layer as the surface will first need to be oxygenated before the metal is added. Ozone is one route to oxygenate the surface and the one which will be used in this project, it is performed by placing the sample into the UV/ozone equipment, in which the UV activates the air to form atomic oxygen which will react with the diamond surface.

1.3.4.3 Metal and Metal-oxide Terminations

The oxygenated surface can become useful in emission by depositing a metal onto this surface. The metal-oxide termination will provide a positive dipole on the outermost layer of the surface, given the chosen metal is relatively electropositive. It may also be a NEA surface.

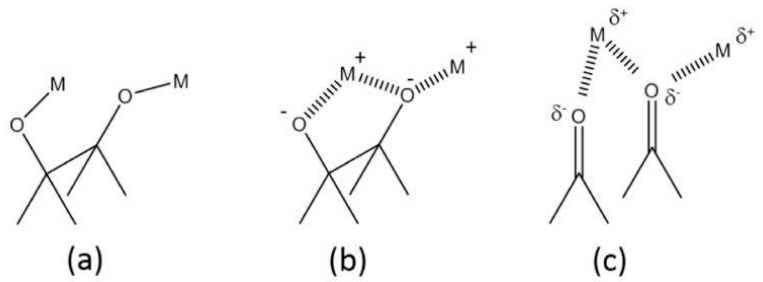

Figure 10 - Different bonding of metals, to the oxygenated surface. (a) covalently bonded, (b) ionically bonded and (c) dipole interactions[40]. M shows the metal and O the oxygen which is bonded to carbon on the diamond surface.

Metal oxides have been known to also decrease the work function of diamond. The absorption of caesium onto the oxygenated surface can reduce the work function of the material from 5.5 eV to 1.25 eV, however this surface isn't stable at high temperatures and would not withstand those used in thermionic emission[46]. The Cs-O scheme was one of those first investigated, it led to the understanding that smaller elements needed to be investigated to improve thermal stability.

Lithium was then a clear candidate to explore for emission devices. It can be deposited onto either clean diamond or the oxygenated surface, Li is a small metal which can bind well to the diamond surface. It was found to be of similar stability to that of the hydrogen-terminated diamond and provide a larger negative electron affinity[47].

Magnesium was shown to give a large NEA, -2.0 eV on the oxygen-diamond surface. It doesn't require the thermal activation that the lithium surface does and shows good promise for emission devices[48].

1.3.4.4 Transition Metal Terminations

Transition metal oxides (TMOs) present a new area of research into finding the best surface termination. This will be one that is thermally stable, lowers the work function whilst maintaining the all-important NEA. These factors will keep the energy barrier for emission low and allow for an efficient emitter.

Diamond surfaces terminated with an ultra-thin TMO layer have been found to cause a noticeably negative shift in the electron affinity. These reactions are exothermic, and the product is incredibly

stable at higher temperatures compared to those available in the alkali metal oxide terminations[49].

Table 1 summarises the transition metals which have currently been investigated for emission purposes and shows that some may be viable emitter surfaces when the most favourable stoichiometry is used.

Table 1 - Calculated electron affinities and absorption energies for transition metals absorbed onto an oxygenated surface[42]. Modifications taken from Jane Geldard[50].

Transition Metal	M:O	Surface Reconstruction 2 x *N*	Adsorption Energy (eV)	Electron Affinity (eV)	Pauling Electronegativity
Ti	1:1	1	-5.35	1.74	1.54
	1:2	1	-6.15	1.57	
	1:4	**2**	**-7.60**	**-3.10**	
Ni	1:1	2	-2.67	1.41	1.91
	1:2	**1**	**-3.80**	**-0.16**	
	1:4	2	-2.69	1.67	
Cu	1:1	1	-2.05	0.05	1.90
	1:2	**1**	**-2.35**	**-1.28**	
	1:4	2	0.03	1.13	
Zn	1:1	1	-1.00	0.30	1.65
	1:2	**1**	**-1.13**	**-3.05**	
	1:4	1	0.97	-0.40	

1.4 Thermionic Emission of Other Materials

1.4.1 Tungsten

Both pure and thoriated tungsten have been investigated for electron emission. Thermionic emission from thoriated tungsten requires the reduction from ThO_2 to Th followed by the diffusion of this metal to the surface. Carbonisation is required to give desirable emission characteristics, the carbonised film; consisting of thorium metal and thorium carbide, is more thermally stable[51].

1.4.2 Lanthanum hexaboride

Rare earth hexaborides, LnB_6 (Ln = La-Lu), hold many good characteristics for use in thermionic emission devices; chemical stability, high melting point, superconductivity, low work function and narrow band semi-conductivity are all considered useful in thermionic emission[52]. CeB_6 has attracted interest due to its hardness, high chemical stability and high electron emission abilities. LaB_6 has also been investigated[53].

LaB_6 can be used as a cathode in thermionic emission devices on account of its low work function, 2.6 eV[52], metallic conductivity and low operating temperature[54]. Emission will be reduced if impurities exist in the crystal, so high-quality crystals of LaB_6 are necessary.

1.5 Scandium

1.5.1 Properties of Scandium

During the discovery of the periodic table by Mendeleev in 1869 a gap was left between Ca and Ti, this was later filled by scandium after its discovery by a Swedish chemist, Nilson, in 1879[55]. Scandium is a group three transition metal and is classified as a rare-earth element[56]. Its low density (2.99 g cm^{-3}) and high melting point (1,538 ˚C) make it suitable for strengthening aluminium alloys, these

are now used in many industries including aerospace and automobile. The ability of scandium to greatly strengthen the alloy even in relatively small quantities is increasing its demand and may lead to potential supply issues.

Scandium has the electronic configuration [Ar]$3d^1 4s^2$ and takes the 3+ oxidation state. It has a small atomic radius, similar to that of magnesium. Scandium has a Pauling electronegativity value of 1.36[55], this has a good difference from that of carbon at 2.55[57].

1.5.2 Scandate Cathodes

Scandate cathodes have attracted interest for thermionic emission processes. Scandium would appear to be a suitable candidate due to its size and high electropositivity. Although many models have been proposed, at present the BaO on Sc_2O_3 model shown in Figure 11 is the one which has been investigated the most. Initial experiments showed this was a stable configuration at high temperatures[58].

Using a scandium oxide termination alone has not yet been trialled and it is only known that the BaO on Sc_2O_3 model shows enhanced emission than that of BaO alone.

1.5.3 Scandium in Thermionic Emission Devices

The properties of scandium make it interesting for uses in thermionic emission devices. It has already been used to improve the performance of barium based cathodes, this was proposed to lower the work function of the material, tungsten in these experiments[59].

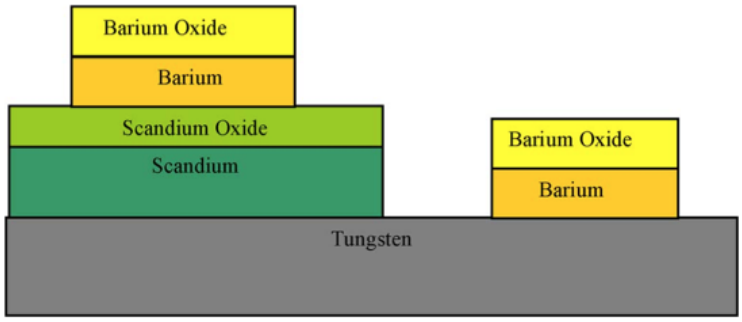

Figure 11 - Demonstration of the films deposited on the tungsten cathode[60].

In summary, the experiments found the best thermionic emission from the Ba/BaO on Sc_2O_3 on tungsten, better than the Ba/BaO alone. High activation temperatures are not required, and the scandium metal diffuses onto W. The Sc_2O_3 won't diffuse at operating temperatures[60].

This report will explore evaporating sub-monolayers of Sc onto single-crystal (100) diamond surfaces, annealing it so that it chemically bonds, and then testing its electron emission performance at different temperatures using a bespoke thermionic-testing apparatus.

1.6 Summary

Work on thermionic emission was on the decline as the techniques were not showing too much promise for energy conversion. New materials and potential surface terminations have increased the interest in thermionic emissions and TECs again. This is promising for the search for a 'greener' energy source[61].

2. Experimental

2.1 Overview

The aim of this experiment was to measure whether emission from Sc-O-terminated diamond was viable and stable under high temperature conditions. Following on from previous work it was predicted the surface termination would provide the NEA and temperature stability necessary.

2.2 Sample preparation

2.2.1 Nitrogen Doping

The nitrogen-doped diamond (NDD) was grown on a molybdenum substrate. The sample had a surface area of 1 cm^2 with a thickness of approximately 500 μm. The incorporation of nitrogen into the diamond emitter is believed to increase emission as the doping provides a donor band below the conduction band minimum. This can be seen more clearly in the diagram shown in Figure 8.

Figure 12 - The MWCVD reactor used in the University of Bristol Diamond lab.

The samples were grown in a MWCVD reactor under 2.45 GHz microwave plasma in a 1.5 kW ASTeX-type reactor, the conditions shown in table 2. The sample is placed inside the reactor and positioned on a tungsten disc on a layer of Mo wire in the centre of the chamber.

Table 2 – Growth conditions for NDD.

Time / mins	90.00
Pressure / Torr	140.70
Power / W	1400.00
Temperature / °C	1121.00
Hydrogen flow / sccm	300.00
Methane flow / sccm	12.50
Nitrogen flow / sccm	0.30

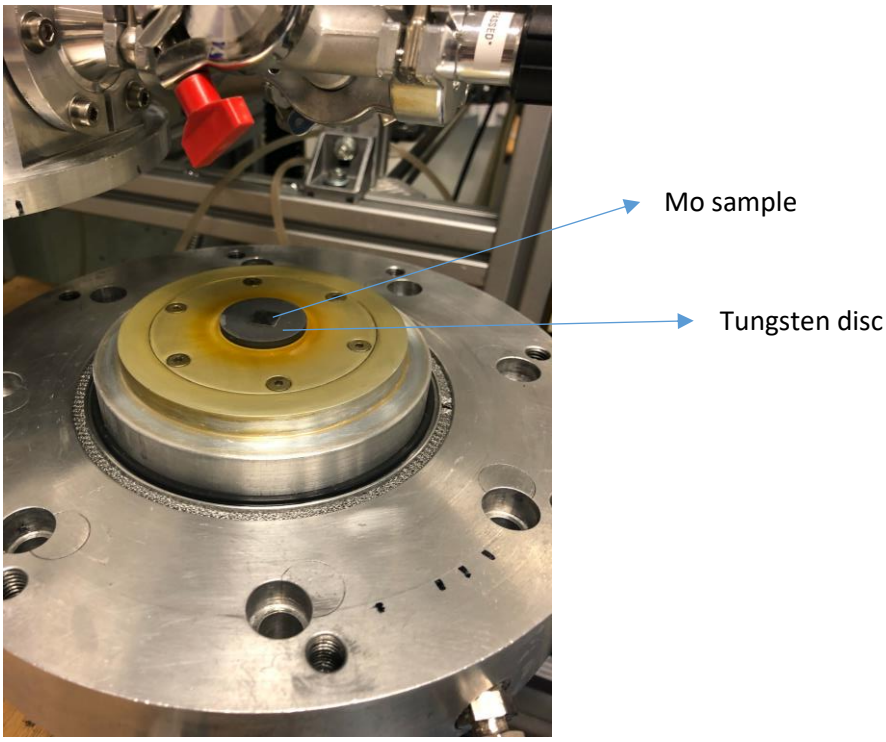

Figure 13 - How the sample sits inside the MWCVD reactor.

2.2.2 Hydrogen Termination

The sample was hydrogen terminated as this is known to possess a NEA and will perform emission, so the sample could be tested before further surface terminations were performed.

Here the sample was placed under a purely hydrogen plasma with a flow rate of 300 sccm (standard cubic centimetres per minute). In a three-step process, the sample becomes hydrogen terminated. The first phase involved cleaning the sample to ensure no other surface terminations or contaminations are present. The second, terminating phase, terminates the surface sites with hydrogen at a lower temperature to prevent desorption. Lastly, the chamber is taken to low power, temperature and pressure in order to extinguish the chamber with the plasma switched off but remaining under hydrogen flow. The conditions for each of these steps are shown in the tables below.

Table 3 – Conditions for H-termination of N-doped diamond.

Step 1 - Cleaning	
Time / mins	2
Pressure / Torr	100.80
Power / W	1000
Hydrogen flow / sccm	300
Temperature / °C	870
Step 2 – Terminating	
Time / mins	2
Pressure / Torr	58.30
Power / W	585
Hydrogen flow / sccm	300
Temperature / °C	556
Step 3 – Extinguishing	
Time / mins	2
Pressure / Torr	32.80
Power / W	0
Hydrogen flow / sccm	300
Temperature / °C	0

2.2.3 Oxygen Termination

The sample needed to be oxygen-terminated before the Sc could be deposited. This was done via the UV/ozone technique. The sample was placed into the chamber, shown in Figure 14, for 30 minutes. This works by UV activating the air passing over the sample to form ozone and atomic oxygen, which reacts with the diamond surface.

Figure 14 - Ozonolysis machine at University of Bristol.

2.2.4 Sc Deposition

The final step necessary for completing the sample preparation is the Sc deposition. For this a Sc rod was used (2 mm diameter $\times$ 28 mm length) as the metal source, and the method used was electron-beam evaporation at room temperature using a degassed Mantis QUAD EV-C evaporator at the base pressure of ~1.0×10^{-9} mbar. A quarter monolayer was deposited (~0.825 Å) of Sc coverage over a timescale of 18 minutes using the NanoESCA system.

2.2.5 Grating

Mo is a refractory metal, with a very high melting point of 2620 ˚C[62] making it stable under the thermionic testing conditions. However, it lacks sufficient optical properties so will not absorb light very well.

The Mo substrate was modified to increase absorption of laser light, by patterning a 10.5 μm grating on the base layer using a laser cutter. This way, the metal will better absorb heat from the IR laser when the thermionic testing is undertaken. This is due to the grating size being similar to the wavelength of the light from the CO_2 heating laser.

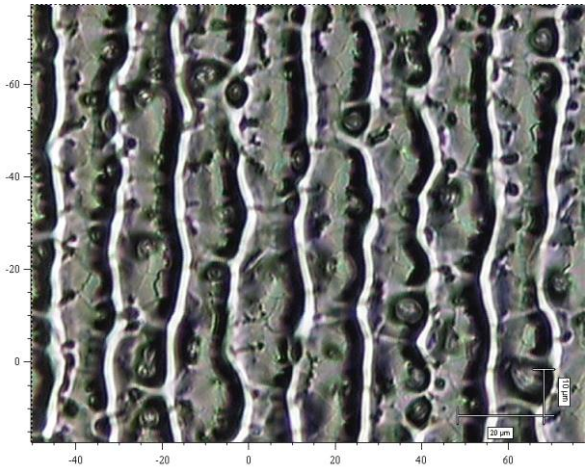

Figure 15 - Mo surface with 10.5 µm laser cutter grating.

2.3 Thermionic studies

The thermionic energy converter testing kit uses controlled laser heating under pressure to measure the thermionic emission of a material. For both H and ScO terminations, five profiles were achieved so that temperature could be plotted against current. The distance between the emitter and collector was also remotely controlled for accurate knowledge of the distance.

The patterned back side of the Mo substrate was heated using a CO_2 laser, with a wavelength of $\lambda = 10.6$ μm and a maximum power output of 40 W. The laser light was absorbed by the patterned Mo grid and converted into heat. The collector was made of tungsten, which has the highest melting point of all metals, making it stable under the high temperature conditions. A pyrometer was in place, as shown in Figure 16, in order to measure the temperature accurately throughout the electrode separation.

Figure 16 - Thermionic testing equipment in the University of Bristol Diamond lab.

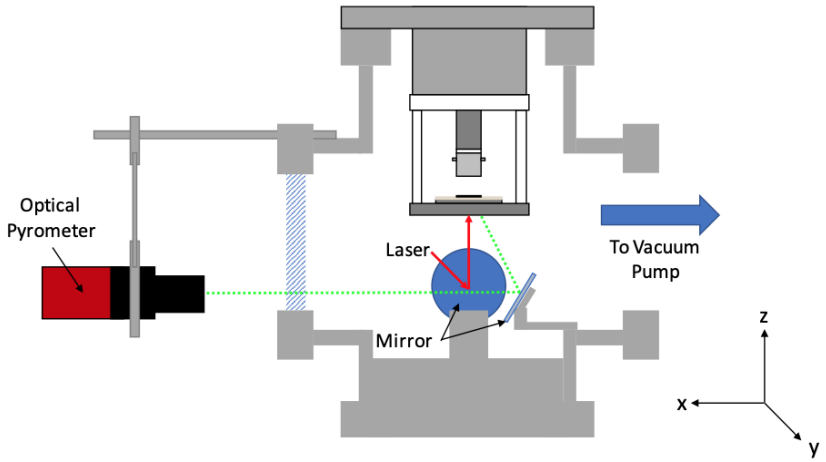

Figure 17 - Schematic of the TEC internally[63]. (Adapted from A. Rowan thesis).

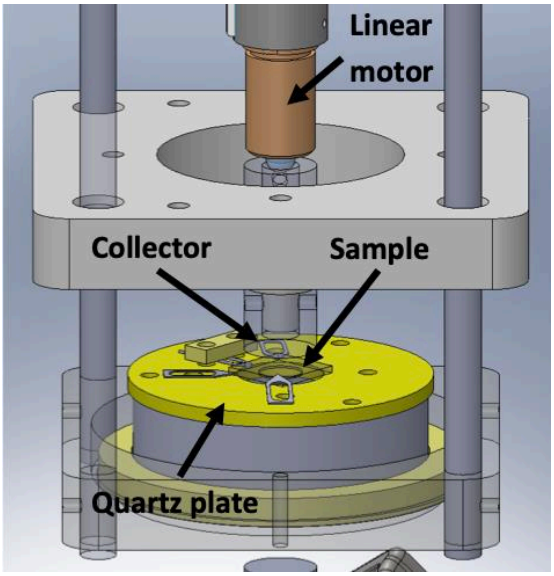

Figure 18 - Inside of the TEC, showing a magnified region of the emitter and collector[64]. (Taken from H. Andrade thesis).

2.3.1 H-terminated Diamond

For the hydrogen-terminated sample, temperature ramping of 1 ˚C per second was used from 300 ˚C to 750 ˚C; the temperature cannot exceed this to prevent rapid desorption of hydrogen from the surface.

Table 4 – Conditions for H-terminated thermionic testing.

Pressure / mbar	10^{-7}
Voltage / volts	25
Distance / μm	200
Emissivity / ems	0.125

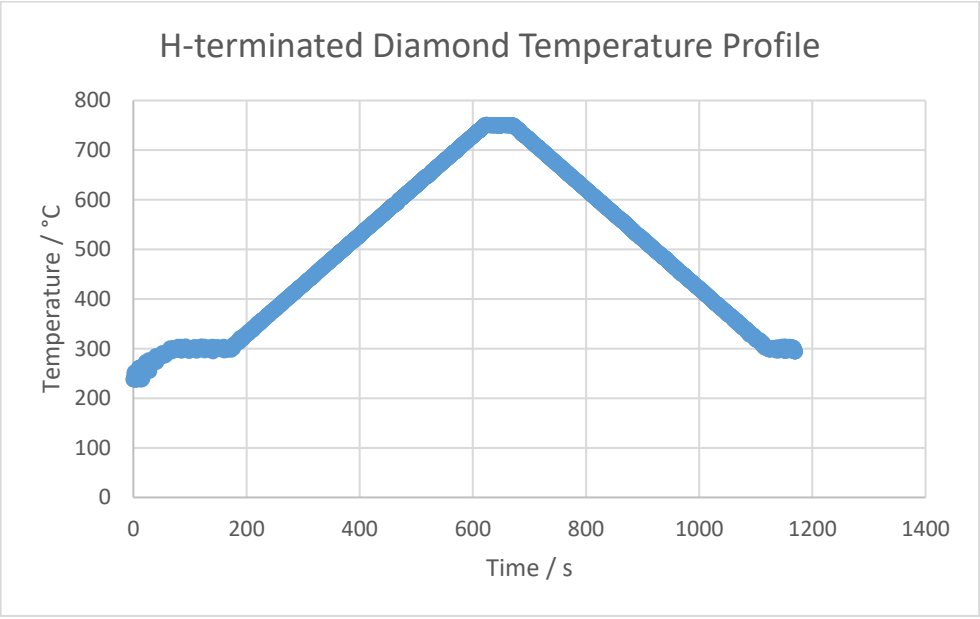

Figure 19 - Temperature profile of the H-terminated sample during a profile.

2.3.2 Sc-O-terminated Diamond

During the testing of the Sc-O-terminated diamond, temperature ramping of 1 ˚C per second was used from 300 ˚C to 900 ˚C for the first profile and from 300 ˚C to 850 ˚C for the following four profiles. A higher temperature could be trialled for the Sc-O-terminated samples as desorption was not expected at such low temperatures.

Table 5 – Conditions for Sc-O-terminated thermionic testing.

Pressure / mbar	10^{-7}
Voltage / volts	25
Distance / μm	150
Emissivity / ems	0.125

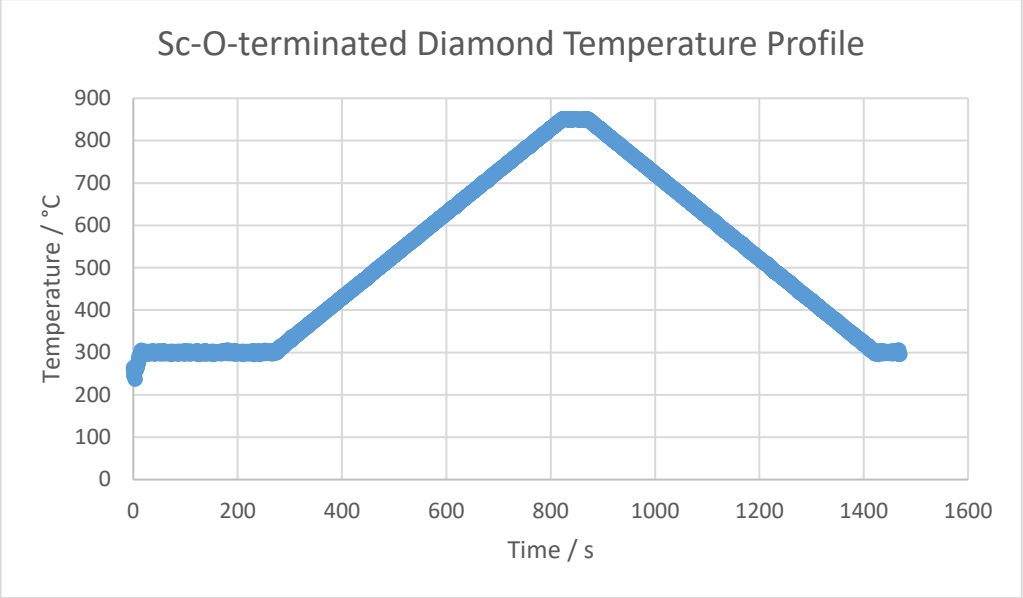

Figure 20 - Temperature profile of Sc-O-terminated sample during a profile.

2.4 Sample Characterisation

Using both laser Raman spectroscopy and scanning electron microscopy (SEM), the samples grown could be analysed and the surface investigated.

2.4.1 Raman

Raman spectroscopy could be used to see if diamond growth has been successful. Here the clear peak at ~1332 cm^{-1} is characteristic of diamond.

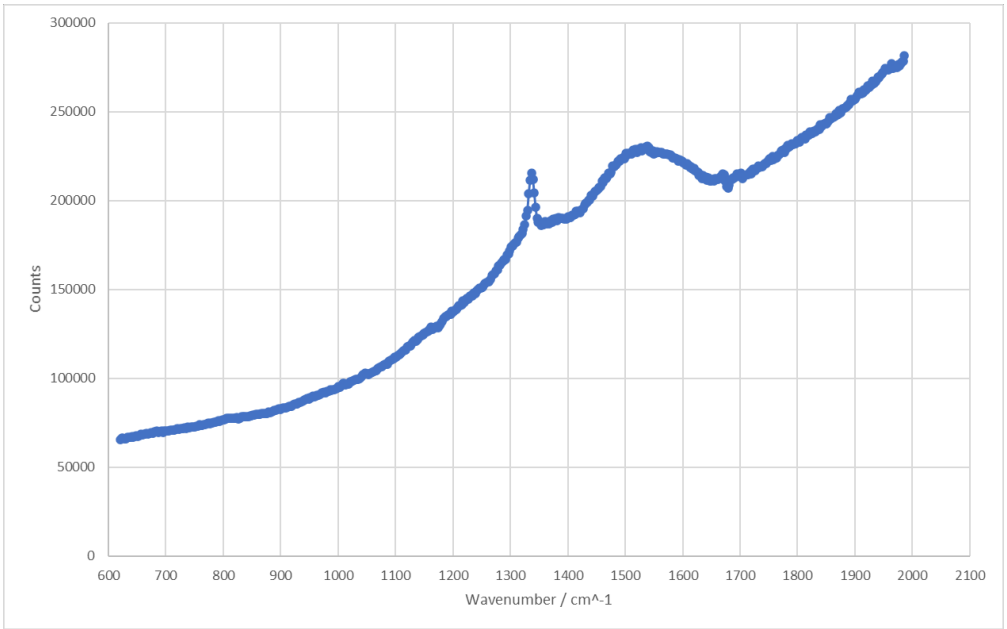

Figure 21 - Raman spectra for N-doped diamond on Mo (1 hour growth).

Figure 22 - Raman system in the University of Bristol Diamond lab.

2.4.2 Scanning Electron Microscopy

SEM was used to check the appearance of the surface structure. Below are several images of the diamond surface. Figure 23 shows the surface taken from angles of 0 ° and 70 °. Figure 24 shows a cross sectional image of the sample. From these a good, even growth coverage is visible.

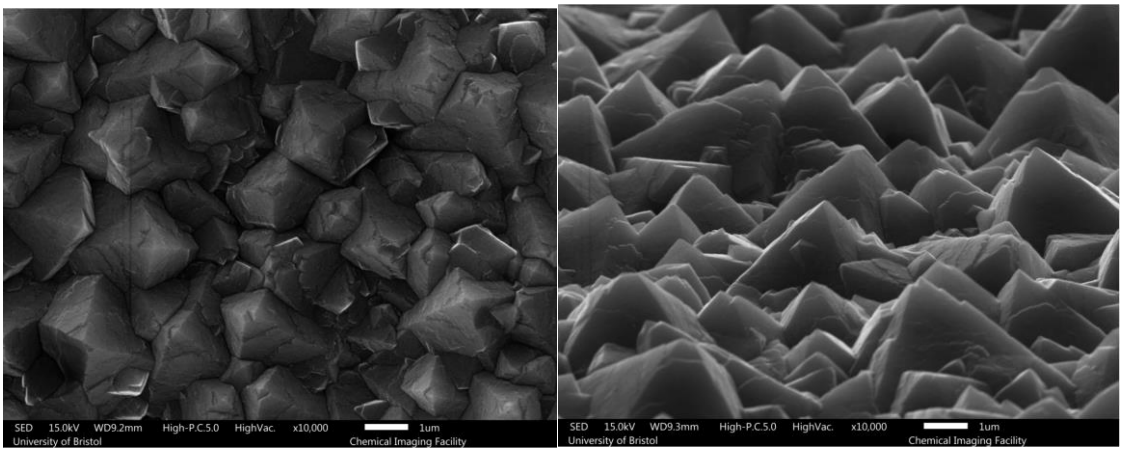

Figure 23 - Surface of the diamond from 0 ° *(*left) and 70 ° (right).

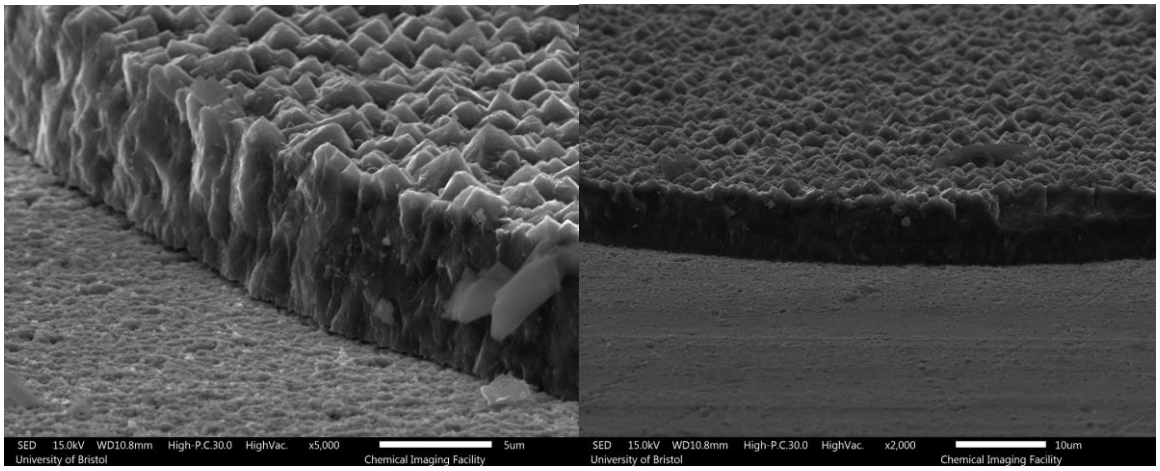

Figure 24 - Cross sectional images of N-doped diamond on Mo (1 hour growth).

3. Results

Here the emission from both the H-terminated and Sc-O-terminated species will be discussed.

3.1 Maximum Current

For both terminations, a maximum current was achieved in each profile. Subsequent profiles of the H-terminated sample showed an overall decrease in maximum emission, whereas for the Sc-O-terminated sample successive profiles showed that the maximum emission varied very little and even showed an overall increase.

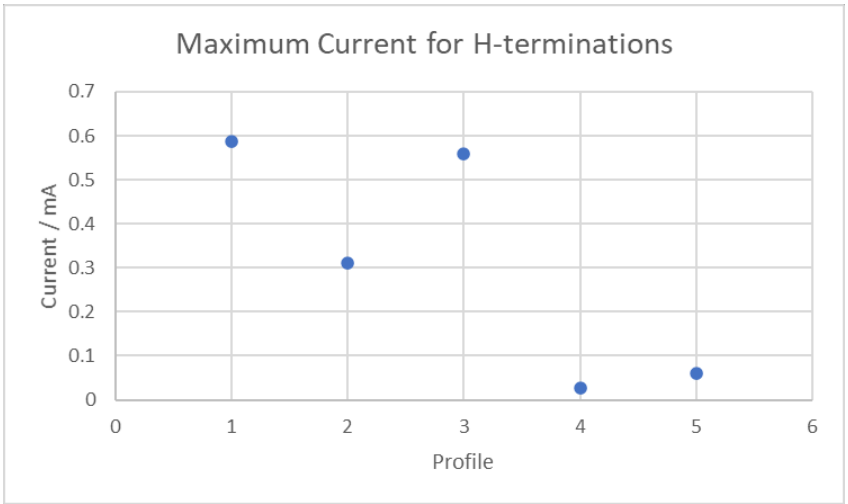

Figure 25 - Peak emission current for successive H-terminated diamond profiles.

As visible from Figure 25 the maximum current observed from the H-terminated diamond decreased over successive thermionic emission profiles. Knowing that hydrogen will desorb from the surface at temperatures as low as 600 °C, this was expected, as the sample was not H-terminated again between profiles and a maximum temperature of 750 °C was used. This is further evidence that the H-terminated sample is not sufficiently temperature stable, and a better surface termination needs to be investigated.

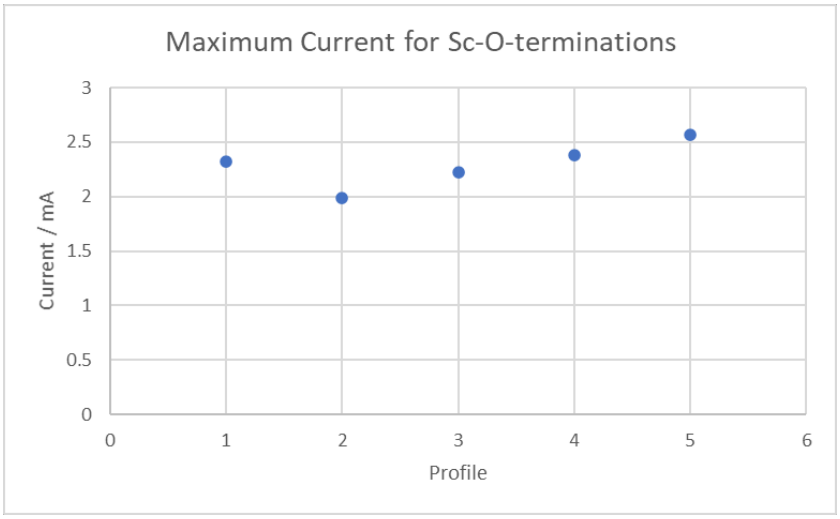

Figure 26 - Peak emission current for successive Sc-O-terminated diamond profiles.

In contrast to the results for the H-terminated sample the Sc-O-terminated sample maintains similar maximum emission values for all profiles and even experiences a steady increase from the second to fifth profile. This suggests the emission can be maintained at high temperatures and the termination

is viable for use. It is also clear from comparing these two graphs (Figure 25 and Figure 26) that overall emission is much higher in every profile of the Sc-O-terminated sample.

3.2 Heating runs

3.2.1 H-terminated-NDD on Mo

In order to ensure the sample was capable of emission before the Sc-O termination was performed, the sample was first hydrogen terminated and emission was measured in the thermionic energy converter.

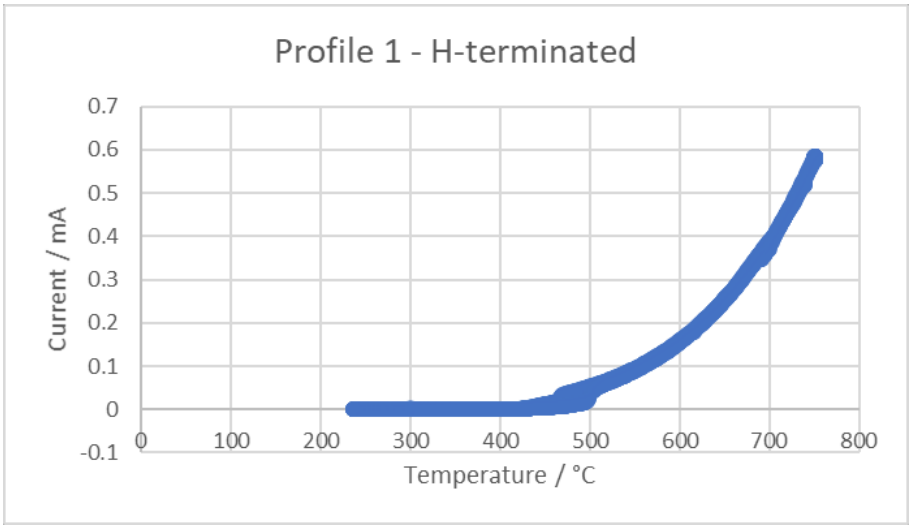

Figure 27 - Profile 1 of H-terminated NDD on Mo at 200 µm.

Once a temperature threshold of 377 ˚C was achieved the sample began to emit electrons. The first profile showed the highest emission of all the H-terminated samples, reaching a peak at 0.586 mA, with a corresponding temperature of 751 ˚C.

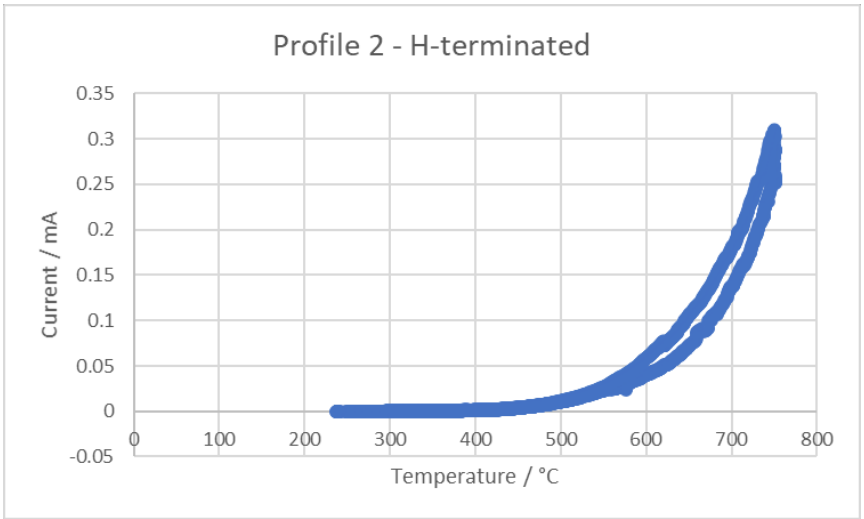

Figure 28 - Profile 2 of H-terminated NDD on Mo at 200 µm.

The temperature threshold for emission was lower for the second profile, at 329 ˚C. This is most likely as the sample was not left to cool, instead the ramping profile was restarted very soon after the first. As expected, emission was lower, with the maximum current at 0.31 mA. This is consistent with the desorption of the hydrogen at high temperatures.

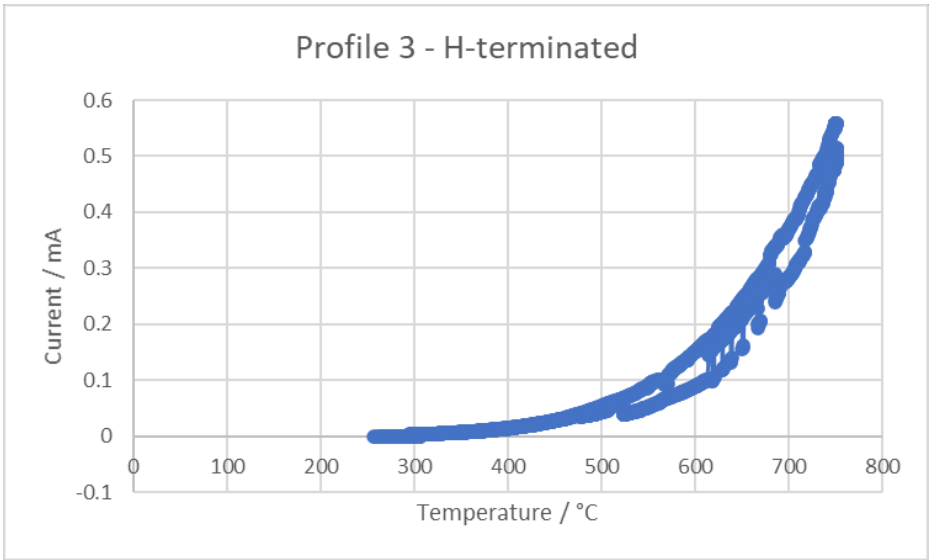

Figure 29 - Profile 3 of H-terminated NDD on Mo at 200 µm.

Interestingly profile 3 showed an increased maximum emission from profile 2, with a value of 0.559 mA, making it closer to the first. However, the profile was a lot more disordered with several big drops in emission. The variation could be due to the hydrogen surface being partially desorbed. The main region which experienced rapid drops in emission is between 600-700 °C, this is above the threshold at which it is known hydrogen readily desorbs from the surface.

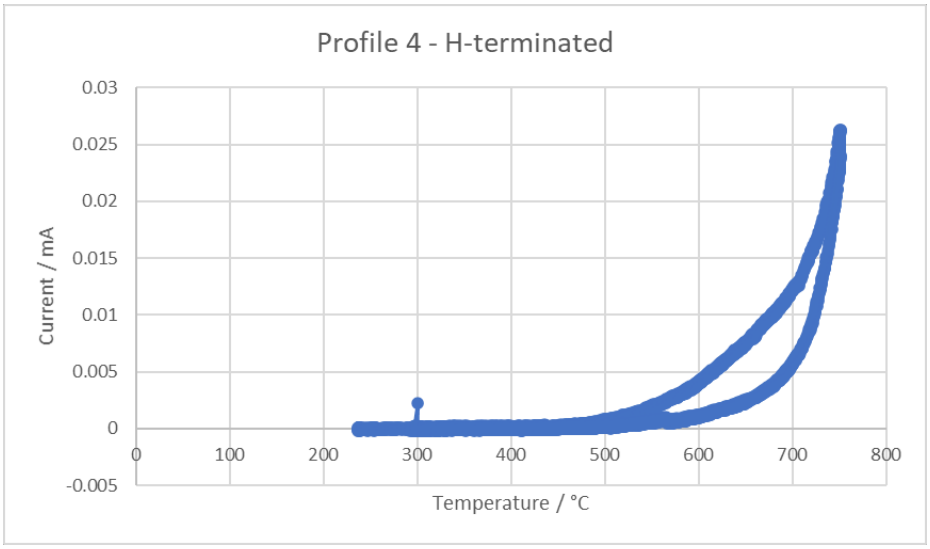

Figure 30 - Profile 4 of H-terminated NDD on Mo at 200 µm.

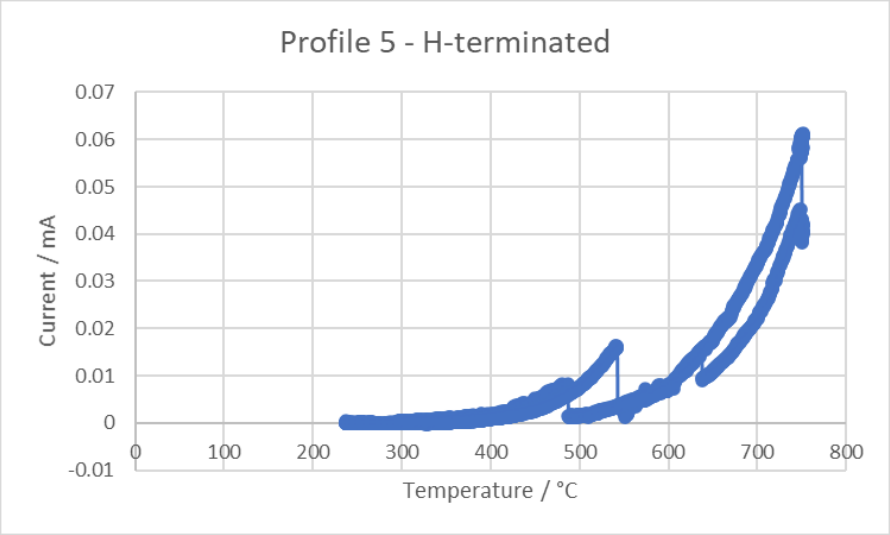

Figure 31 - Profile 5 of H-terminated NDD on Mo at 200 µm.

For both profiles 4 and 5, the maximum current was significantly lower with 0.0263 mA and 0.0612 mA, respectively. This shows that by the time these profiles took place the surface had been severely affected by the repeated high temperatures and that a fully hydrogenated surface termination no longer remained. Focusing on the fifth profile, a first drop in emission is observed just below 500 °C and a further huge drop in emission is observed between 500 – 600 °C. This shows reasonable evidence for the sample lacking thermal stability in the later profiles.

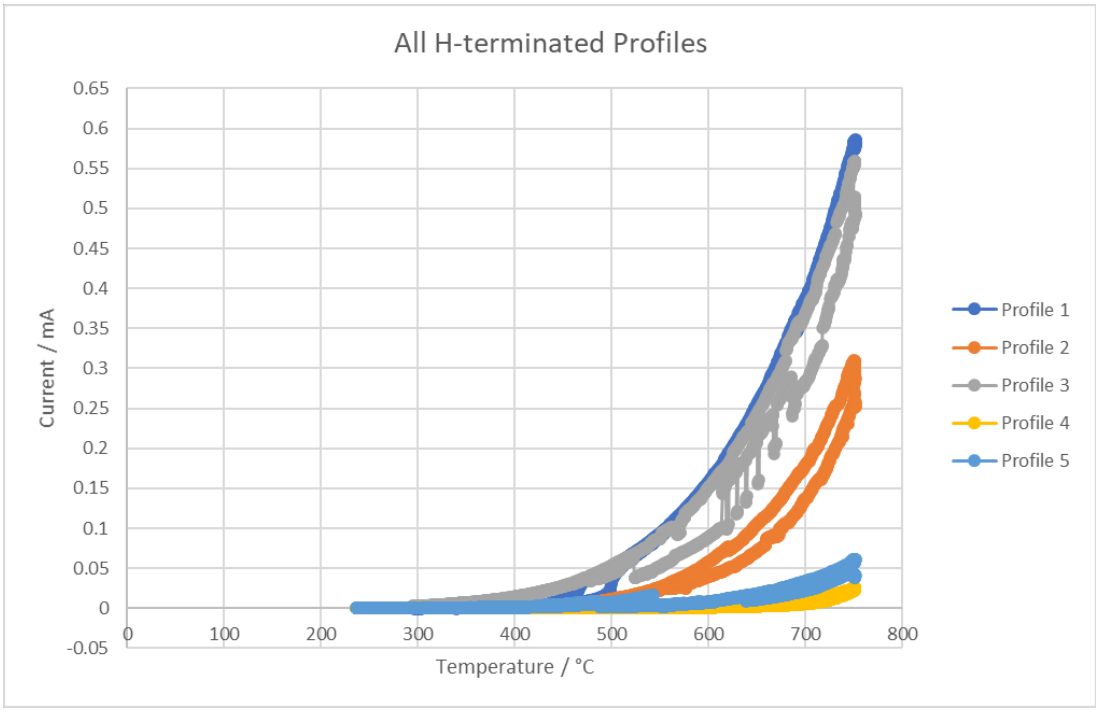

Figure 32 - All H-terminated NDD on Mo profiles.

Plotting all these profiles onto one graph allows for even better comparison of the data. Here it is evident how the emission decreases throughout successive profiles and the big difference in maximum current between the first and last testing is very evident.

3.2.2 ScO-terminated-NDD on Mo

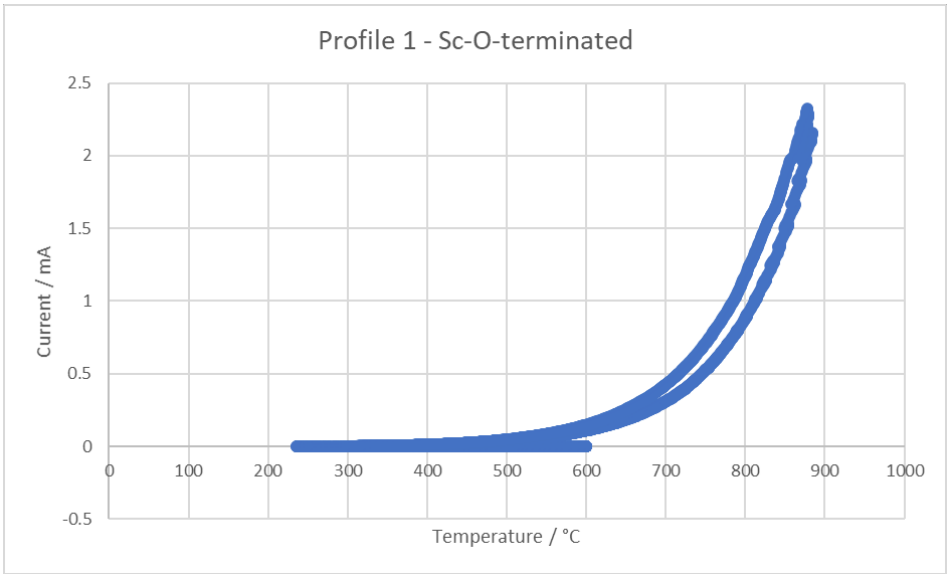

Figure 33 - Profile 1 of Sc-O-terminated NDD on Mo at 150 µm.

Immediately from the profiles of the Sc-O-terminated sample it is evident that these provide better emission than a freshly H-terminated sample. During the first profile, a maximum current of 2.323 mA was reached, more than 5 times the first and largest of the hydrogen-terminated results.

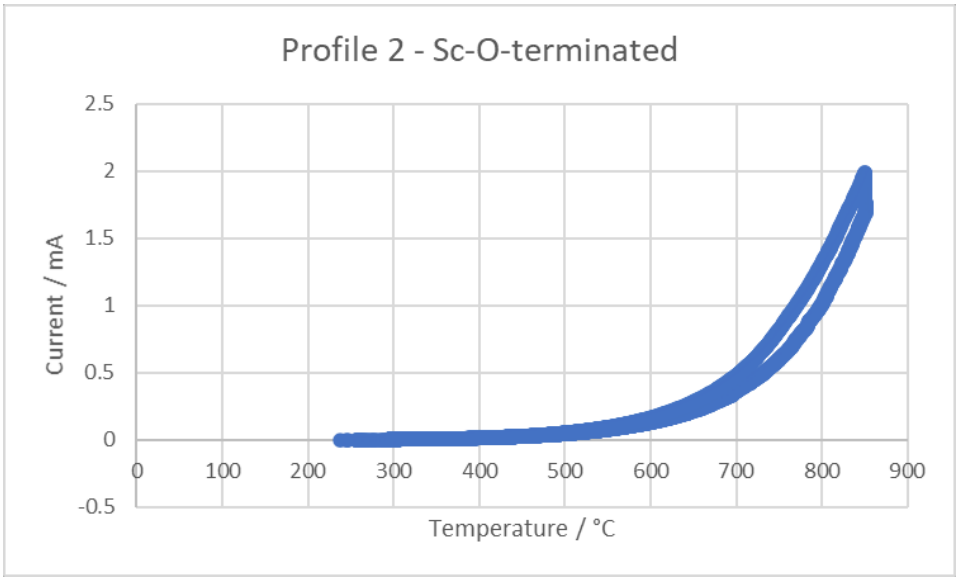

Figure 34 - Profile 2 of Sc-O-terminated NDD on Mo at 150 µm.

The second profile for this termination did not show a large decrease in the maximum and produced another similar clean emission profile.

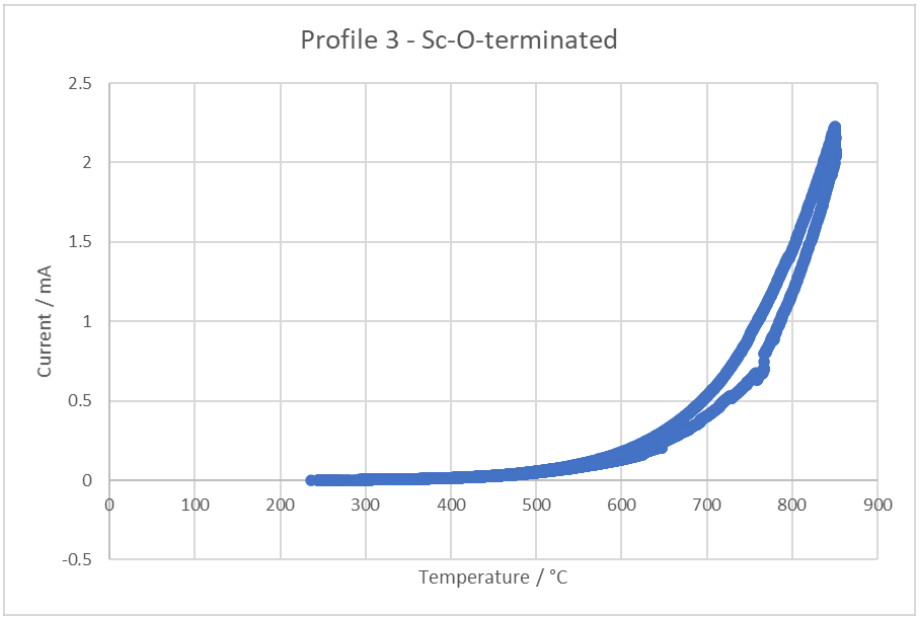

Figure 35 - Profile 3 of Sc-O-terminated NDD on Mo at 150 µm.

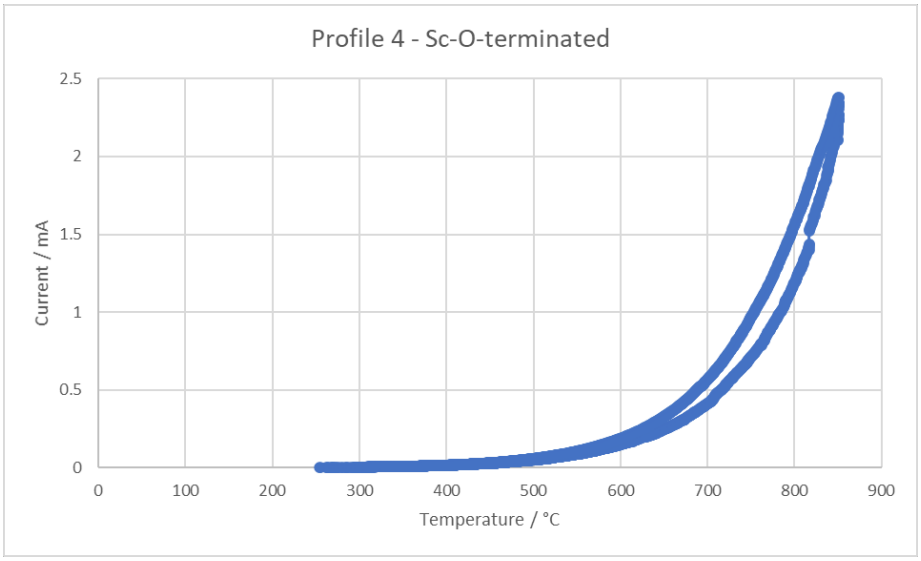

Figure 36 - Profile 4 of Sc-O-terminated NDD on Mo at 150 µm.

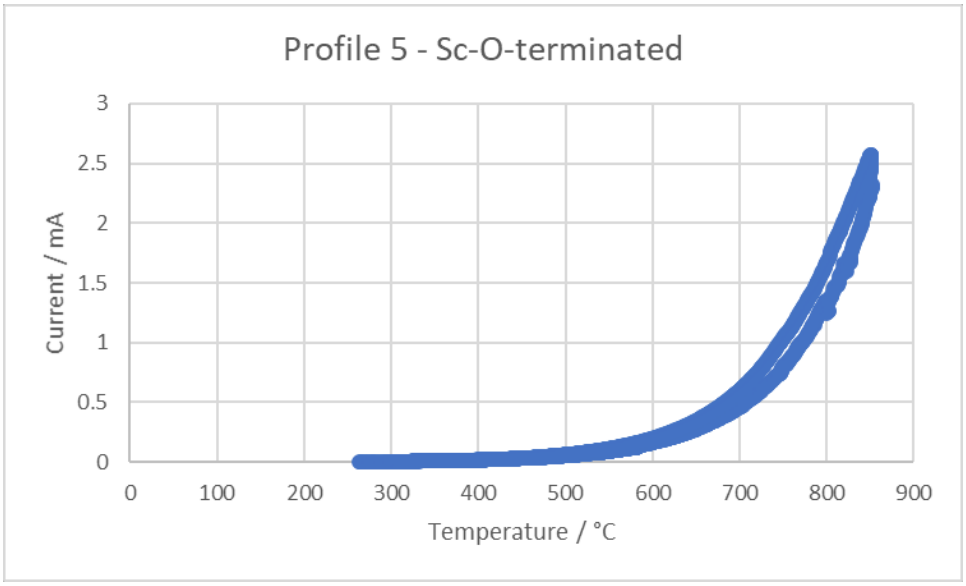

Figure 37 - Profile 5 of Sc-O-terminated NDD on Mo at 150 µm.

The successive three emission profiles for the Sc-O-terminated samples (Figure 35, Figure 36 and Figure 37) showed a steady increase in maximum emission and in the fifth profile the highest maximum was reached at 2.569 mA at 851 °C, providing evidence that the sample is temperature stable and will continue to produce good and reliable emissions at high temperatures, notably higher than those of the hydrogen-terminated sample.

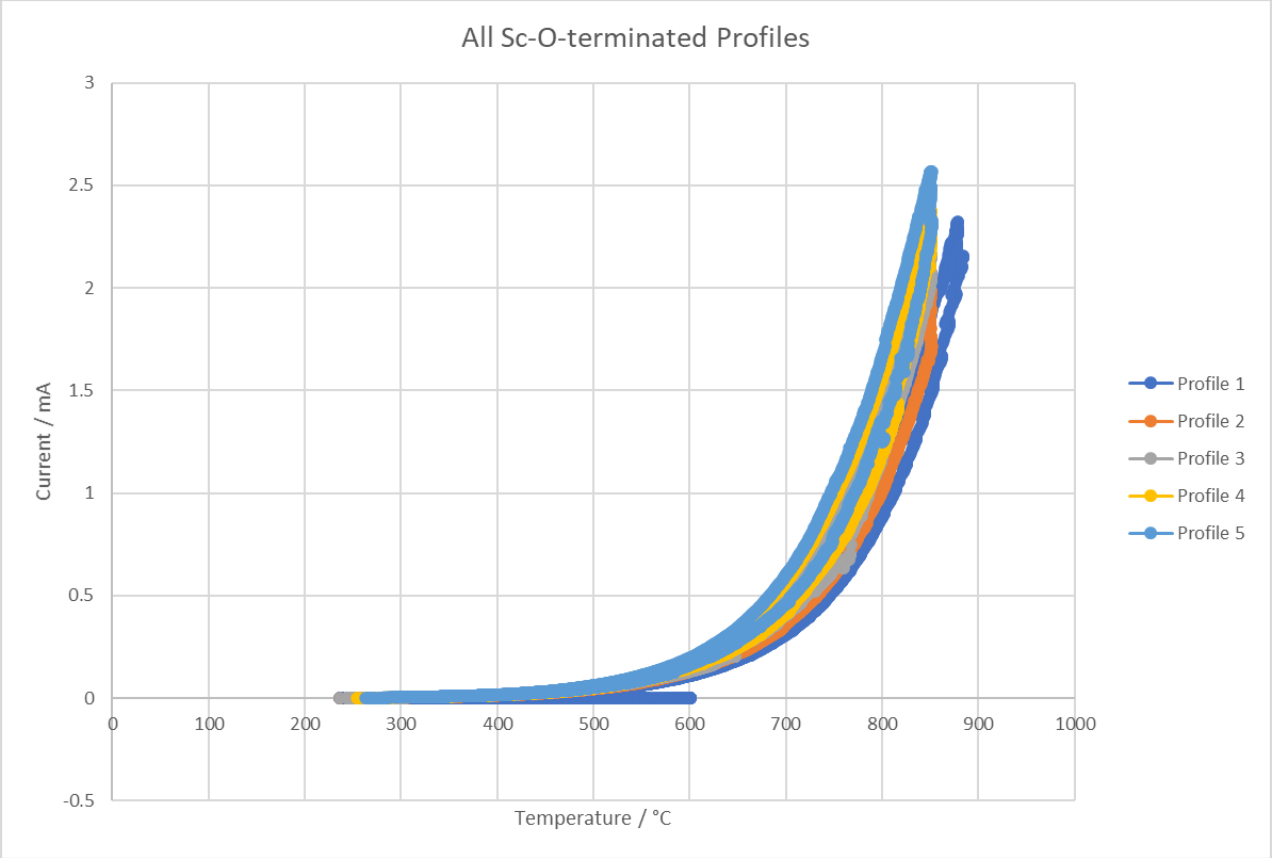

Figure 38 - All Sc-O-terminated profiles.

Comparing all the Sc-O-terminated profiles, it is very evident that the profiles are more consistent, and the surface remains stable without desorption.

3.3 The Collector

Throughout the time in the lab there were issues with the collector, and several were trialled. The one which was used for the data collected was a tungsten collector. This collector was the most reliable and could manage the high temperatures used in the experiments.

3.4 Cathode-Anode Distance

The distance between the electrodes can have a significant effect on emission. During the H-terminated sample profiles a larger distance of 200 μm was used. The Sc-O-terminated sample testing was performed at 150 μm. The distance used is significant as it can have an influence on the space-charge effect, in future testing it may be better to have both comparable tests at the same distance as the H-terminated sample may have performed slightly better at a shorter distance, as smaller distances are known to limit the space-charge effect.

4. Conclusion

The two samples were tested for their ability to increase the thermionic emission properties of diamond by lowering the work function and providing a NEA surface. There was already evidence for a H-terminated sample providing these conditions and this termination was mostly done to ensure the sample had good emission properties once the nitrogen doping and backside grating had been performed.

The Sc-O-terminated sample was expected to have good emission characteristics based on other metal-oxide terminations which have been performed. Scandium's size, ability to become highly charged and electropositivity all suggested the sample would emit successfully and this was found when its thermionic emission abilities were studied.

The Raman data shows good diamond growth due to the peak at 1332 cm^{-1} and SEM images show good diamond growth on the surface of the Mo, all the evidence suggests the sample, once Sc-O-terminated has the ability to be a successful emitter.

Bibliography

[1] V. Robinson, et al, *Diamond and Related Materials*, 2006, **15**, 1601-1608.
[2] J. Johnson, *American Journal of Physics*, 1960, **28**, 763-773.
[3] P. Redhead, *Journal of Vacuum Science & Technology A*, 1998, **12**, 1396.
[4] T. Jones, *Thermionic Emission*, Methuen & Co, London, 1936.
[5] A. Reiman, *Thermionic Emission*, Chapman & Hall, London, 1934.
[6] C. Crowell, *The Richardson Constant for Thermionic Emission in Schottky Barrier Diodes*, 1965, **8**, 395-399.
[7] A. Vijh, P. Lenfant, *Canadian Journal of Physics*, 1973, **51**, 111-113.
[8] J. Houston, H. Webster, *Thermionic Energy Conversion*, 1963, **17**, 125-206.
[9] K. Khalid, T. Leong, K. Mohamed, *Review on Thermionic Energy Converters*, 2016, **63**, 2231-2239.
[10] K. Jensen, *Journal of Applied Physics*, 2007, **102**, 024911-5.
[11] S. Dushman, *Electron Emission from Metals as a Function of Temperature*, 1923, **21**, 623-631.
[12] J. Lee, et al, *Journal of Microelectromechanical Systems*, 2014, **23**, 1182-1187.
[13] J. Smith, et al, *Journal of Vacuum Science and Technology B*, 2009, **27**, 1132-1135.
[14] D. De, et al, *Highly Improved Thermionic Energy Converter*, 2019, **1378**, 1-11.
[15] T. Ito, M. Cappelli, *Applied Physics Letters*, 2012, **101**, 213901.
[16] N. Rasor, *Emission Physics of the Thermionic Energy Converter*, 1963, **5**, 733-747.
[17] I. Lim, S. Lambert, J. Vay, et al, *Applied Physics Letters*, 2018, **112**, 073906.
[18] J. Lee, I. Bargatin, N. Melosh, et al, *Applied Physics Letters*, 2012, **100**, 173904.
[19] J. Ristein, *AIP Conference Proceedings*, 2005, **772**, 377-380.
[20] C. Wu, A. Kahn, *Journal of Applied Physics*, 1999, **86**, 3209.
[21] M. Campbell, T. Celenza, et al, *Progress Toward High Power Output in Thermionic Energy Converters*, 2021, **9**, 1-23.
[22] B. Moyzhes, T. Geballe, *Journal of Applied Physics*, 2005, **38**, 782-786.
[23] J. Houston, *Journal of Applied Physics*, 1959, **30**, 481-486.
[24] K. Jensen, Y. Lau, N. Jordan, *Applied Physics Letters*, 2006, **88**, 164105.
[25] M. Islam, O. Inal, J. Luke, *Journal of Applied Physics*, 2006, **100**, 084903.
[26] J. Schwede, et al, *Nature Materials*, 2010, **9**, 762-766.
[27] A. Kribus, G. Segev, *Journal of Optics*, 2016, **18**, 73001.
[28] M. Ramalingam, T. Young, *Mechanical Engineering CIME*, 1993, **115**, 78.
[29] P. May, *Diamond Thin Films: A 21st Century Material*, 2000, **358**, 473-495.
[30] S. Kidalv, F. Shakhov, *Thermal Conductivity of Diamond Composites*, 2009, **2**, 2467-2495.
[31] C. Wort, R. Balmer, *Materials Today*, 2008, **11**, 22-28.
[32] D. Takeuchi, H. Kato, G. Ri, et al, *Applied Physics Letters*, 2005, **86**, 152103.
[33] S. Ferro, *Journal of Materials Chemistry*, 2002, **12**, 2843-2855.
[34] P. Cannon, *Journal of the American Chemical Society*, 1962, **84**, 4253-4256.
[35] J. Luong, K. Male, J. Glennon, *Boron-doped Diamond Electrode; Synthesis, Characterisation, Functionalistion and Analytical Applications*, 2009, **134**, 1965-1979.
[36] J. Gracio, et al, *Journal of Applied Physics D*, 2010, **43**, 1-22.
[37] R. Kalish, *Doping of Diamond*, 1999, **37**, 781-785.
[38] K. Thonke, *Semiconductor Science and Technology*, 2003, **18**, S20-S26.
[39] J. Birrell, J. Gerbi, O. Auciello, et al, *Journal of Applied Physics*, 2003, **93**, 5605-5612.
[40] M. James, F. Fogarty, R. Zulkharnay, et al, *A Review on Surface Functionalisation of Diamond for Thermionic Emission Applications*, 2021, **171**, 532-550.
[41] K. O'Donnel, T. Martin, N. Allan, *Light Metals on Oxygen-Terminated Diamond (100): Structure and Electronic Properties*, 2015, **27**, 1306-1315.

[42] A. Tiwari, J. Goss, P. Briddon, et al, *Physical Review B*, 2011, **84**, 245305.
[43] I. Krainsky, V. Asnin, *Applied Physics Letters*, 1998, **72**, 2574.
[44] Y. Guo, et al, *IOP Conference Series: Materials Science and Engineering*, 2018, **452**, 1-5.
[45] D. Petrini, K. Larsson, *The Journal of Physical Chemistry C*, 2007, **111**, 795-801.
[46] K. O'Donnell, T. Martin, N. Fox, D. Cherns, *Physical Review B*, 2010, **82**, 11503.
[47] S. Ullah, L. Cullingford, T. Zhang, et al, *An Investigation into the Surface Termination and Near-surface Bulk Doping of Oxygen-terminated Diamond with Lithium at Various Annealing Temperatures*, 2021, **6**, 311-320.
[48] K. O'Donnell, et al, *Physical Review B*, 2015, **92**, 35303.
[49] A. Tiwari, et al, *Unexpected Change in the Electron Affinity of Diamond Caused by the Ultra-Thin Transition Metal Oxide Films*, 2014, **108**, 46005.
[50] J. Geldard, *Metal Oxide Termination as a Route to Low Work Function Surfaces*, 2019.
[51] P. Schneider, *Journal of Chemical Physics*, 1958, **28**, 675-682.
[52] X. Ji, Q. Zhang, J. Xu, Y. Zhao, *Progress in Solid State Chemistry*, 2011, **39**, 51-69.
[53] S.Ning, T. Iitaka, X. Yang, Y. Wang,J. Zhao, Z. Li, J. Zhang, *Journal of Alloys and Compounds*, 2018, **760**, 1-5.
[54] M. Futamoto, M. Nalazawa, K. Usami, et al, *Journal of Applied Physics*, 1980, **51**, 3869-3876.
[55] A. William-Jones, O. Vasyukova, *The Economic Geology of Scandium, the Runt of the Rare Earth Element Litter*, 2018, **4**, 973-988.
[56] A. Botelho, D. Espinosa, J. Vaughan, J. Tenorio, *Minerals Engineering*, 2021, **172**, 107148.
[57] W. Gordy, J. Thomas, *Journal of Chemical Physics*, 1956, **24**, 439-441.
[58] G. Lensy, R. Forman, *Surface Studies on Scandate Cathodes and Synthesised Scandates*, 1990, **37**, 2595-2604.
[59] M. Mroz, S. Tenney, T. Savina, et al, *AIP Advances*, 2018, **8**, 65114.
[60] J. Vaughn, K. Jamison, M. Kordesch, *In Situ Emission Microscopy of Scandium/ Scandium-Oxide and Barium/ Barium-Oxide Thin Films on Tungsten*, 2009, **56**, 794-798.
[61] G. Xiao, G. Zheng, M. Qiu, Q. Li, D. Li, M. Ni, *Applied Energy*, 2017, **208**, 1318-1342.
[62] N. Rasor, J. McClelland, *Thermal Properties of Graphite, Molybdenum and Tantalum to Their Destructive Temperatures*, 1960, **15**, 17-26.
[63] A. Rowan, Thesis, University of Bristol, 2019.
[64] H. Andrade, Thesis, University of Bristol, 2019.